Electronic supplementary information (ESI)

Two novel organic phosphorous-based MOFs: synthesis, characterization and photocatalytic properties

Tianyu Zeng, Liwen Wang, Lu Feng, Hailong Xu, Qingrong Cheng* and Zhiquan Pan*

Key Laboratory for Green Chemical Process of Ministry of Education, Wuhan Institute of Technology, Wuhan 430073, P. R. China

Corresponding authors:

*(Q.C.) E-mail: chengqr383121@sina.com

*(Z.P.) E-mail: zhiqpan@163.com

Total number of pages: 12

Total number of Schemes: 1

Total number of Tables: 4

Total number of Figures: 11

Physical Measurements

The C, H, N microanalyses were performed with a Vario EL elemental analyzer. Fourier-transform infrared spectra (FT-IR) were got using a Bio-Rad FTS6000 spectrophotometer in the wavelength range of 4000 - 400 cm^{-1} (KBr pellets). Thermogravimetric analysis (TGA) were measured on a STA 409 PC analyzer in the temperature range of 30 - 900 °C with a heating rate of 10 °C min^{-1} under nitrogen flow. The powder X-ray diffraction (PXRD) experiments were carried out on Rigaku D-MAX2550 (λ = 0.15417 nm) with 2θ ranging from 5° to 80° under ambient conditions. The UV-Vis spectrums for the solid state sample were obtained on a HITACHI U-4100 spectrophotometer. The X-ray photoelectron spectra (XPS) were recorded on an ESCALAB250 spectrometer (Thermo-VG Scientific) using Mg Kα radiation (1253.6 eV) and the binding energy values were calibrated with respect to the C (1 s) peak (284.6 eV). Fluorescence spectra were recorded on an F-7000 FL Spectrophotometer with a quartz cuvette (path length = 1 cm). N_2 adsorption-desorption isotherms of the prepared samples at 77 K were measured to investigate the pore textural natures using a surface area analyzer (ASAP 2460, Micromeritics). The pH values were determined by using a pH detector (Rex Instrument, Shanghai, China). ICP-OES results were obtained on Optima 5300DV from Perkin Elmer. The electron spin resonance (ESR)spectra were detected by using a Bruker EPR A 300-10/12 spectrometer to measure the activated species.

Materials and Methods

All reagents and solvents were used as received from commercial suppliers without further purification. 4,4'-Bis(chloromethyl)-1,1'-biphenyl, triethyl phosphite, 4,4'-bipyridine (99.00%), cupric acetate monohydrate (99.00%) and cobalt (II) acetate tetrahydrate (99.00%) were purchased from Sinopharm Chemical Reagent Co., Ltd. Ultrapure water from a Millipore Milli-Q system was used to prepare aqueous solutions for the two complexes synthesis and for the degradation experiments.

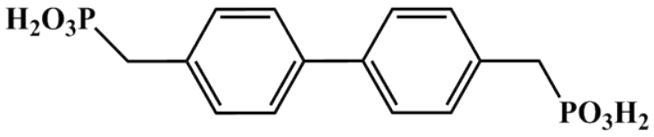

Scheme S1. The structures of ligand H_4L.

Analysis of Chromium (VI) reduction

Cr(VI) concentrations were measured using the 1,5-diphenylcarbazide(DPC) colorimetric method by monitoring the purple complex at 540 nm on a UV-vis spectrophotometer. The specific operation for measurement is as follows: In a 50 mL volumetric flask, 2 mL of sample was mixed with 0.5 mL of H_2SO_4 solution (H_2SO_4: H_2O=1:1) and 0.5mL of H_2PO_4 solution (H_2PO_4: H_2O=1:1). After adding water to the constant volume, 0.2 mL of freshly prepared 0.25% (w/v) DPC in acetone was added to the volumetric flask. The mixture was then shaken for about 15-30 s and allowed to stand for 10-15 min (for full color development). The red-violet to purple color was measured and the absorbance at 540 nm was denoted as Ai (i represents different reaction time intervals).

Experiment of Photoluminescence Spectra (PL)

•OH radical reactions were performed as follows. 4.00 mg of the photocatalyst was suspended in 40.0 mL aqueous solution containing 2.00×10^{-3} M NaOH and 5.00×10^{-4} M terephthalic acid. Before exposure to light, the suspension was stirred in the dark for 1 h. And then 1.00 mL sample was removed every 10 min and centrifuged for fluorescence spectroscopy measurements. A fluorescence spectrophotometer was used to measure the fluorescence signal of the 2-hydroxy terephthalic acid generated. The excitation light wavelength used in recording fluorescence spectra was 320 nm and the emission wavelenght appeared to be ~426 nm.

Radical Trapping Experiments

The radical trapping experiments just have one more additional procedure than the MB photocatalytic process: 10 mM radical scavenger need to be added to the system of photogradation before 125 W mercury lamp turned on at room temperature. The specific dosage of t-BuOH, TEOA and NBT are 38.0 μL, 53.0 μL, and 10mM respectively. The MB concentration changes were monitored by measuring the absorption intensity at its maximum absorbance wavelength of λ = 664 nm using a UV-visible spectrophotometer.

Table S1. Crystallographic data for complexes **1** and **2**

Empirical fomula (Formula weight)	$C_{19}H_{20}CuNO_7P_2$ *(499.84)*	$C_{19}H_{24}CoNO_{9.5}P_2$ *(539.26)*
CCDC deposit no.	1872673	1872661
Temperature/K	173	297
Crystal system	Square pyramidal	monoctahedron
Space group	P	P 2_1/c
a / Å	10.9957(8)	16.6555(15)
b / Å	13.1434(10)	5.7443(5)
c / Å	15.1707(13)	22.1480(16)
α / °	72.061(3)	90
β / °	82.134(3)	94.497(5)
γ / °	66.169(2)	90
V/Å^3	1907.9(3)	2112.5(3)
Z	4	4
D $_{calc}$/g cm^{-3}	1.740	1.696
μ /mm^{-1}	1.358	8.321
F(000)	1024.0	1112.0
h, k, l max	13,15,18	17,5,22
No. of parameters	541	317
S	1.019	1.076
R_1, wR_2 [I > 2σ(I)]	0.0605, 0.0796	0.0729, 0.1787
Δρ max/e Å	0.745	0.745
Δρ min/e Å	0.657	0.607

Table S2. Selected bond distances (A°) and angles (º) for complex **1** and **2**

1		**2**	
Bond lengths (A°)		**Bond lengths (A°)**	
Cu1-O2	1.940(3)	Co1-O4	2.041(5)
Cu1-O1	1.972(5)	Co1-O1	2.064(7)
Cu1-O4	1.981(3)	Co1-O7	2.074(8)
Cu1-N1	2.072(5)	Co1-O8	2.123(8)
Cu1-O7	2.226(4)	Co1-N1	2.142(8)
Cu2-O13	1.894(4)	Co1-O10	2.218(11)
Cu2-O8	1.915(3)	Co1-O3'	2.240(10)
Cu2-O12	1.979(4)		
Cu2-N2	2.004(5)		
Cu2-O14	2.323(5)		
Bond angles (º)		**Bond angles (º)**	
O2-Cu1-O1	89.03(15)	O4-Co1-O1	88.53(24)
O2-Cu1- O4	166.95(16)	O4-Co1-O7	96.00(28)
O1-Cu1- O4	88.03(17)	O4-Co1-O8	88.46(24)
O2-Cu1-N1	90.65(17)	O4-Co1-N1	91.00(24)
O1-Cu1-N1	159.64(18)	O4-Co1-O10	156.36(32)
O4-Cu1-N1	87.72(19)	O4-Co1- O3'	168.05(28)
O2-Cu1-O7	99.25(15)	O1-Co1-O7	175.30(30)
O1-Cu1-O7	103.28(15)	O1-Co1-O8	94.22(27)
O4-Cu1-O7	93.79(15)	O1-Co1-N1	90.46(25)
N1-Cu1-O7	96.86(18)	O1-Co1-O10	78.41(34)
O13-Cu2-O8	172.77(20)	O1-Co1- O3'	97.85(32)
O13-Cu2- O12	93.48(18)	O7-Co1-O8	84.68(33)
O8-Cu2- O12	89.58(17)	O7-Co1-N1	90.71(31)
O13-Cu2-N2	85.26(20)	O7-Co1-O10	96.91(38)
O8-Cu2-N2	89.39(19)	O7-Co1- O3'	77.92(34)
O12-Cu2-N2	157.29(16)	O8-Co1-N1	175.27(33)
O13-Cu2-O14	93.10(19)	O8-Co1-O10	73.16(33)
O8-Cu2-O14	93.20(17)	O8-Co1- O3'	101.06(33)
O12-Cu2-O14	94.31(15)	N1-Co1-O10	108.53(33)
N2-Cu2-O14	108.40(17)	N1-Co -O3'	78.92(32)
		O10-Co1- O3'	35.58(37)

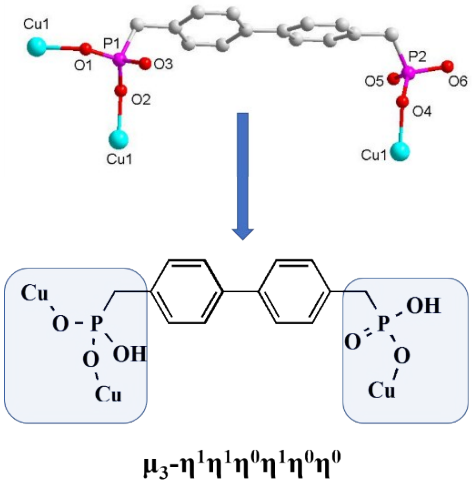

Fig. S1. Coordination mode of the ligand in complex **1**

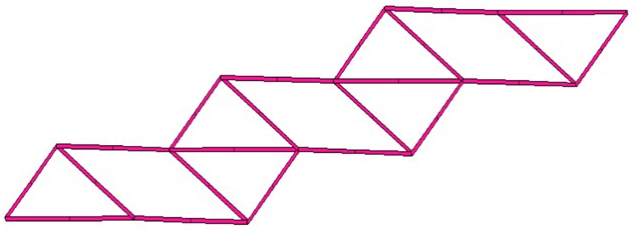

Fig. S2. Topological representation of the network of complex **1**

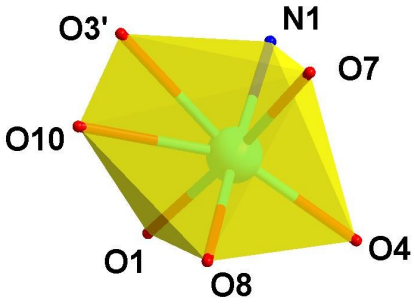

Fig. S3. the coordination environment of Co(Ⅱ) in complex **2**

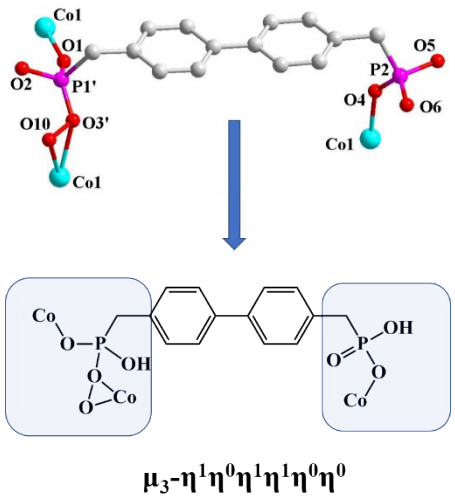

μ_3-$\eta^1\eta^0\eta^1\eta^1\eta^0\eta^0$

Fig. S4. Coordination mode of the ligand in complex **2**

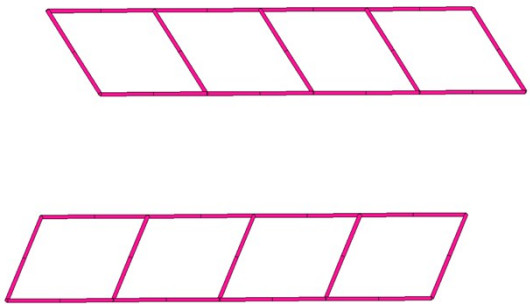

Fig. S5. Topological representation of the network of complex **2**

Table S3. Specific surface areas, pore volumes and mean pore diameters for all samples.

Sample	1	2
Specific surface area (m^2g^{-1})	4.920	23.13
Pore volume ($cm^3\ g^{-1}$)	0.02070	0.1103
Adsorption average pore diameter (nm)	16.85	19.08
Desorption average pore diameter (nm)	3.232	7.065

Table S4. The ICP result of centre metal ions concentration in MB aqueous solution after photocatalysis

System	*ICP result*	*removal rate*
With complex **1**	0.460 mg/L	0.360%
With complex **2**	1.98 mg/L	1.80%

Photocatalyst: 40 mg; MB: 40 mL, 10 ppm.

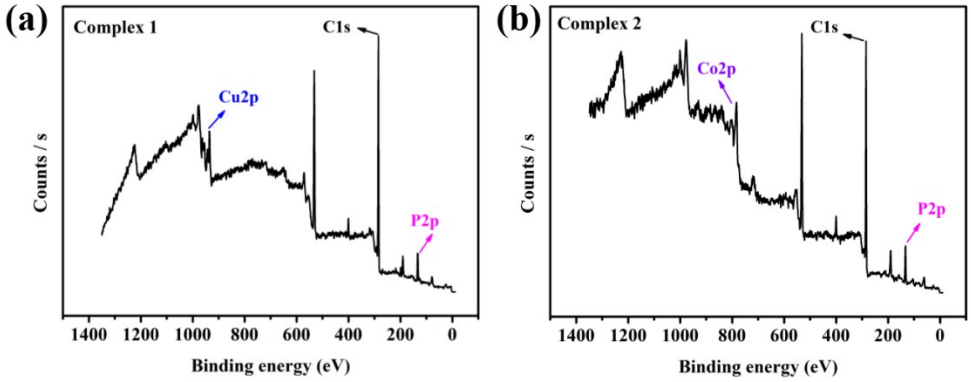

Fig. S6 XPS spectra for complexes **1** (a) and **2** (b) after photocatalytic degradation of MB: survey spectrum.

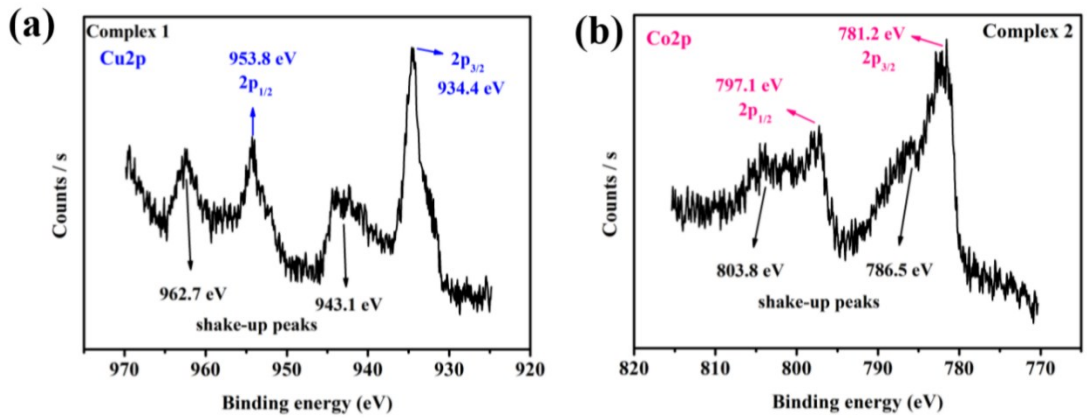

Fig. S7 (a) Cu 2p spectrum bound to complex **1** after photocatalysis; (b) Co 2p spectrum bound to complex **2** after photocatalysis.

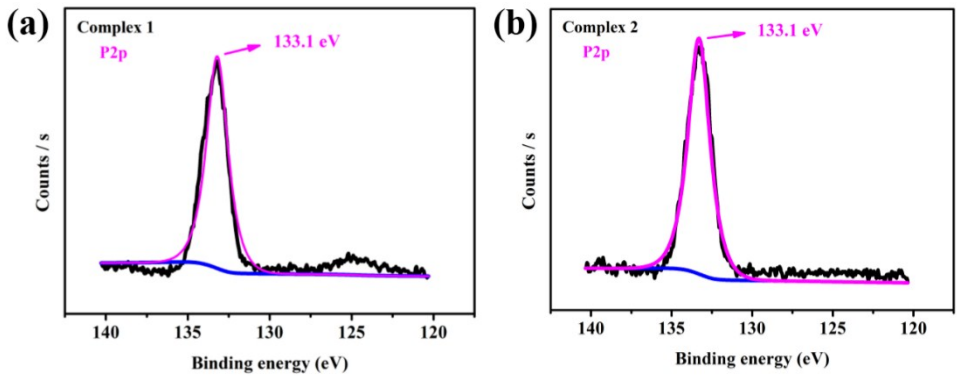

Fig. S8 P 2p spectrum bound to complexes **1** (a) and **2** (b) after photocatalysis

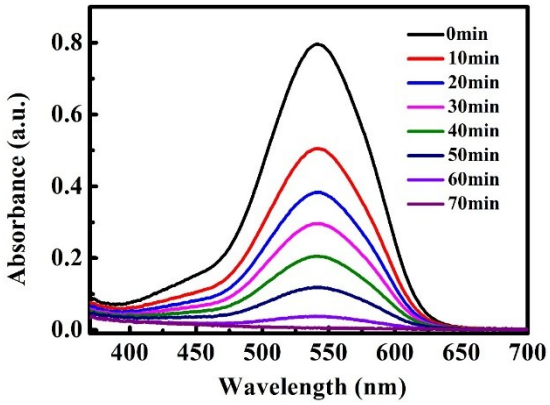

Fig. S9. Time-dependent absorption spectra for the photocatalytic reduction of aqueous Cr(VI) over complex **1**.

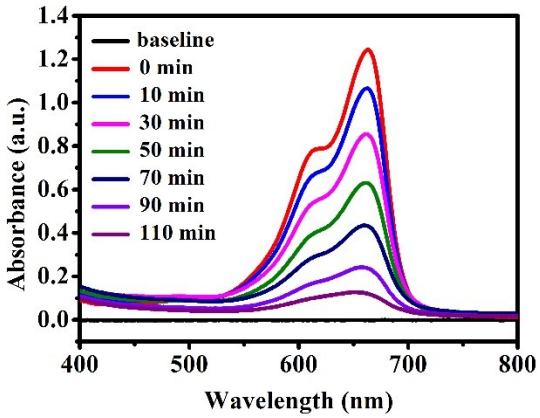

Fig. S10. Time-dependent absorption spectra for the photocatalytic degradation of MB over complex **2**.

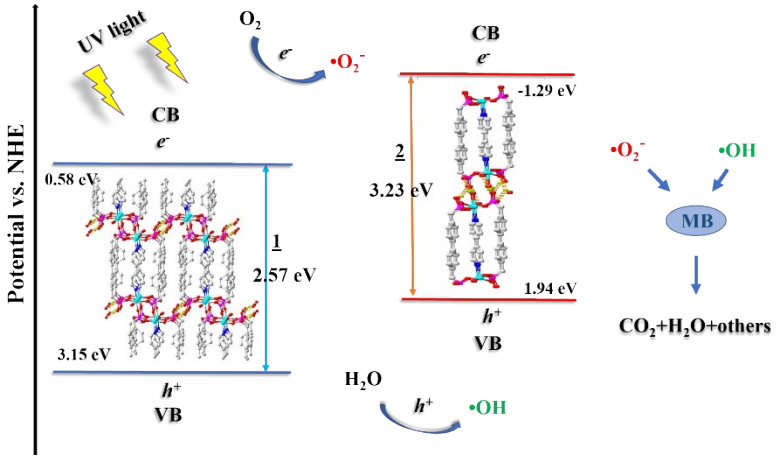

Fig S11. A schematic illustration of the energy position and photocatalytic degradation of MB over complexes **1** and **2**.